THE JOURNAL OF PHYSICAL CHEMISTRY B
A JOURNAL OF THE AMERICAN CHEMICAL SOCIETY

pubs.acs.org/JPCB
Article

Ion Association and Hydration of Some Heavy-Metal Nitrate Salts in Aqueous Solution

Johannes Hunger,* Richard Buchner,* and Glenn Hefter*

Cite This: https://doi.org/10.1021/acs.jpcb.4c05441
Read Online

ABSTRACT: Aqueous solutions of four heavy-metal nitrate salts ($AgNO_3$, $TlNO_3$, $Cd(NO_3)_2$ and $Pb(NO_3)_2$) have been studied at 25 °C using broadband dielectric relaxation spectroscopy (DRS) at frequencies $0.27 \leq \nu/\mathrm{GHz} \leq 115$ over the approximate concentration range $0.2 \lesssim c/\mathrm{mol\ L^{-1}} \lesssim 2.0$ ($0.08 \lesssim c/\mathrm{mol\ L^{-1}} \lesssim 0.4$ for the less-soluble $TlNO_3$). The spectra for $AgNO_3$, $TlNO_3$, and $Pb(NO_3)_2$ were best described by assuming the presence of three relaxation processes. These consisted of one solute-related Debye mode centered at ~2 GHz and two higher-frequency solvent-related modes: one an intense Cole−Cole mode centered at ~18 GHz and the other a small-amplitude Debye mode at ~500 GHz. These modes can be assigned, respectively, to the rotational diffusion of contact ion pairs (CIPs), the cooperative relaxation of solvent water molecules, and its preceding fast H-bond flip. For $Cd(NO_3)_2$ solutions an additional solute-related Debye mode of small-amplitude, centered at ~0.5 GHz, was required to adequately fit the spectra. This mode was consistent with the presence of small amounts of solvent-shared ion pairs. Detailed analysis of the solvent modes indicated that all the cations are strongly solvated with, at infinite dilution, effective total hydration numbers (Z_t^0 values) of irrotationally bound water molecules of ~5 for both Ag^+ and Tl^+, ~10 for Pb^{2+}, and ~20 for Cd^{2+}. These results clearly indicate the presence of a partial second hydration shell for $Pb^{2+}(aq)$ and an almost complete second shell for $Cd^{2+}(aq)$. However, the hydration numbers decline considerably with increasing solute concentration due to ion−ion interactions. Association constants for the formation of contact ion pairs indicated weak complexation that varies in the order: $Tl^+ < Ag^+ < Pb^{2+} < Cd^{2+}$, consistent with the charge/radius ratios of the cations and their Gibbs energies of hydration. Where comparisons were possible the present constants mostly agreed well with the rather uncertain literature values.

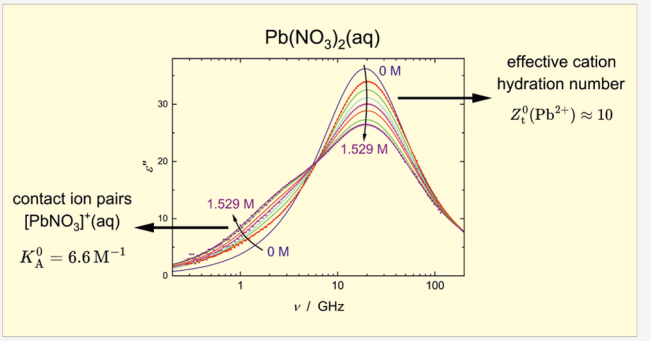

INTRODUCTION

Heavy metal ions and their salts ("heavy metals," HMs) have been the focus of much research over many decades, consistent with their technological, scientific, and even (for some) cultural uses.[1−4] More recently, HMs have attracted interest and concern as ubiquitous and hazardous environmental pollutants spread throughout the planet.[5,6] Nevertheless, despite their importance, compared with most metal ions, relatively little is known about the behavior of these ions in aqueous solution. Of all the properties of electrolyte solutions perhaps the two most important are the extent of hydration of their constituent ions and the level of interaction (association) between those ions. These two properties, which are to some extent competitive, dominate much of the behavior of all electrolyte solutions.

This paper presents a study of the aqueous solutions of four representative heavy-metal nitrate salts: $AgNO_3$, $TlNO_3$, $Cd(NO_3)_2$ and $Pb(NO_3)_2$ using dielectric relaxation spectroscopy (DRS). This technique was chosen because it can provide powerful insights into ion hydration, it is sensitive to the existence of weak ion association, and it has an almost unique ability to quantitatively distinguish the three common types of ion pairs (contact, solvent-shared, and double solvent-separated).[7] Nitrate salts were chosen on the basis of their ready availability in high purity, their good solubilities (with the partial exception of $TlNO_3$) and because the nitrate ion, NO_3^-, being symmetric does not have a net dipole moment and hence does not contribute to the DR spectra, which simplifies their interpretation. Cations were selected because of indications of unusual coordination characteristics.[8−11]

METHODS

Metal salts $AgNO_3$, Carl Roth, p.a. 99.9%; $TlNO_3$, Sigma-Aldrich, 99.999% (trace metals basis); $Cd(NO_3)_2{\cdot}(H_2O)_4$, Sigma-Aldrich, 99.997% (trace metals basis); and $Pb(NO_3)_2$, Sigma-Aldrich, 99.999% (trace metals basis) were used as received. Solutions were prepared by weight without buoyancy

Received: August 13, 2024
Revised: September 19, 2024
Accepted: September 24, 2024

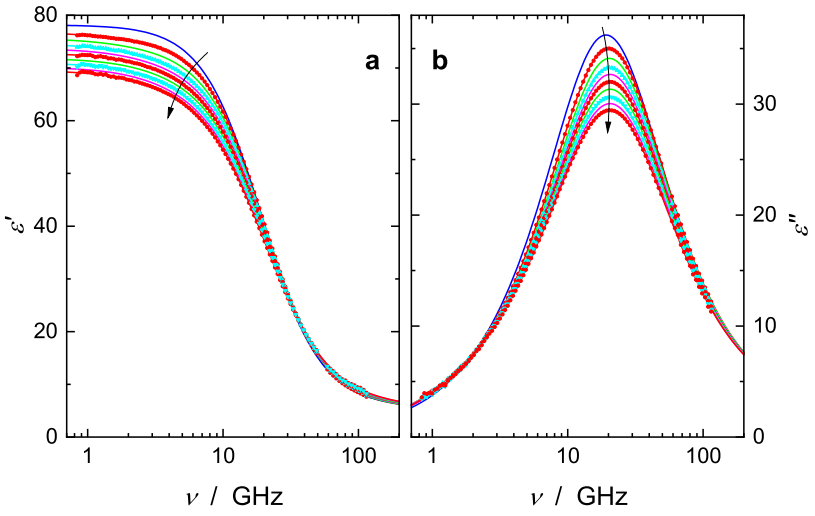

Figure 1. (a) Relative permittivity, $\varepsilon'(\nu)$, and (b) dielectric loss, $\varepsilon''(\nu)$, spectra of aqueous solutions of $AgNO_3$ at 25 °C (symbols) and their fits with the D+CC+D model (lines). Arrows indicate increasing solute concentrations, c/M = 0.204, 0.406, 0.604, 0.799, 1.007, 1.242, 1.502, 1.736, 1.994. Experimental points have been partly omitted for visual clarity. For comparison, the spectrum of neat water (c/M = 0) calculated from the relaxation parameters of Eiberweiser et al.[12] (S_1 = 72.42, τ_1 = 8.35 ps, S_2 = 2.43, τ_2 = 0.278 ps, ε_∞ = 3.52) is also shown.

corrections on an analytical balance, measuring to ±0.1 mg, using high purity deionized water with an electrical resistivity of ≥18 MΩ·cm, drawn from a Millipore line.

Solution densities, ρ, for calculating molar concentrations, c/mol L^{-1} (M), were measured at (25 ± 0.05)°C with an accuracy of ca. 0.1 mg·mL^{-1} using a vibrating-tube densimeter (Mettler Toledo DM40) calibrated with N_2(g) and water, assuming densities from standard sources.[13] The data obtained for the various solutions are included in Tables S1−S4 of the Supporting Information.

Dielectric spectra of total complex permittivity

$$\hat{\eta}(\nu) = \hat{\varepsilon}(\nu) - \mathbf{i}\kappa/(2\pi\nu\varepsilon_0) = \varepsilon'(\nu) - \mathbf{i}[\varepsilon''(\nu) + \kappa/(2\pi\nu\epsilon_0)] \quad (1)$$

were measured as a function of field frequency, ν, using frequency domain reflectometers based on flanged open-ended coaxial probes.[14−16] In eq 1, $\varepsilon'(\nu)$ is the relative permittivity, $\varepsilon''(\nu)$ the dielectric loss, and κ the d.c. conductivity of the sample; ϵ_0 is the electric field constant and $\mathbf{i}^2 = -1$.[17,18] For all samples, frequencies at $0.83 \le \nu/\mathrm{GHz} \le 49$ were recorded using coaxial probes based on 1.85 mm feed-throughs. For Cd$(NO_3)_2$(aq) and Pb$(NO_3)_2$(aq) the range $0.27 \le \nu/\mathrm{GHz} \le 1.25$ was also covered using coaxial probes made from flattened, polished and gold-plated SMA hermetic feed-throughs. Complex scattering parameters were recorded by connecting the coaxial probes to a vector network analyzer (VNA, Anritsu MS4647A). Spectra at $58 \le \nu/\mathrm{GHz} \le 115$ were recorded using a coaxial probe joined with 1 mm connectors to an external frequency converter (Anritsu 3744A mmW) in combination with the VNA.[19] Scattering parameters were corrected for systematic errors using air, conductive silver paint, and water as references.[20] These data were subsequently converted to permittivity spectra using the impedance model described elsewhere.[14,16] The sample temperature was controlled to (25 ± 1)°C by placing it in a silicon oil bath connected to a circulating thermostat (Julabo F12-ED). Spectra were recorded with 5 mL of the sample in a glass vial in contact with the coaxial probes.

For formal description of the spectra so obtained (symbols in Figures 1 and S1−S4), various relaxation models based on the sum of n individual relaxation processes

$$\hat{\eta}(\nu) = \sum_{j=1}^{n} \frac{S_j}{[1 + (\mathrm{i}2\pi\nu\tau_j)^{1-\alpha_j}]^{\beta_j}} + \varepsilon_\infty - \mathrm{i}\kappa/(2\pi\nu\epsilon_0) \quad (2)$$

were tested using a nonlinear least-squares routine that simultaneously fitted $\varepsilon'(\nu)$ and $\varepsilon''(\nu)$. In eq 2, ε_∞ is the high-frequency permittivity of the sample, which is nominally determined only by intramolecular polarizability. Individual dispersion steps, j (in order of increasing peak frequency), of amplitude S_j, and relaxation time τ_j, were modeled by a Havriliak−Negami (HN) equation with relaxation-time distribution parameters $0 \le \alpha_j < 1$ and $0 < \beta_j \le 1$, or its simplified variants: the Cole−Davidson (CD, $\alpha_j = 0$), Cole−Cole (CC, $\beta_j = 1$) or Debye (D, $\alpha_j = 0$, $\beta_j = 1$) equations.[18] The static permittivity of the sample is given by $\varepsilon = \sum S_j + \varepsilon_\infty$. Note that in this procedure κ was also treated as an adjustable parameter.

All reasonable models with $n \le 5$ were tested and the fits obtained, with their parameters, were scrutinized along the lines described elsewhere.[21] It was found that for the dielectric spectra of $AgNO_3$(aq), $TlNO_3$(aq) and Pb$(NO_3)_2$(aq) a D+CC+D model provided the best fit, combining a dominant Cole−Cole mode with $\nu_2^{\mathrm{peak}} = (2\pi\tau_2)^{-1} \approx 18$ GHz, and two weak Debye contributions at $\nu_1^{\mathrm{peak}} \approx 2$ GHz and $\nu_3^{\mathrm{peak}} \approx 500$ GHz (see Figure 2 as a typical example). For Cd$(NO_3)_2$(aq) a D+D+CC+D model with two weak-to-moderate intensity Debye contributions at ∼0.6 and ∼1.5 GHz provided a superior fit (Figure 3). As discussed below, for all samples the highest-frequency mode can be associated with the fast H-bond flip of solvent water molecules,[22] although the notable increase in its amplitude for Pb$(NO_3)_2$(aq) (Table S3) and Cd$(NO_3)_2$(aq) (Table S4) may point to additional contributions from ions rattling in their solvent cages.[23] As this contribution is centered outside the covered frequency range, its relaxation time (0.278 ps) and ε_∞ (3.52), were fixed in the overall fit to values obtained from the spectrum of neat water extending to 2000 GHz.[12] The fit parameters obtained are summarized in Tables S1−S4, while the fits are shown as lines in Figures 1 and S1−S4.

https://doi.org/10.1021/acs.jpcb.4c05441
J. Phys. Chem. B XXXX, XXX, XXX−XXX

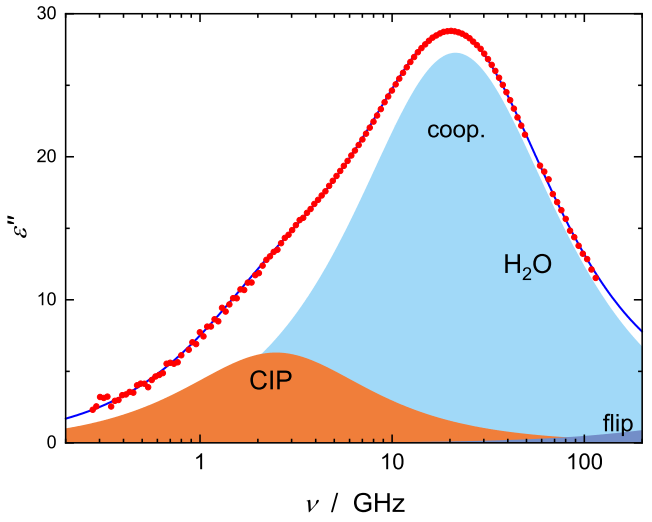

Figure 2. Dielectric loss, $\varepsilon''(\nu)$, spectrum of a 1.029 M aqueous solution of $Pb(NO_3)_2$ at 25 °C (symbols) and its fit with the D+CC+D model (line). Shaded areas indicate the contributions due to contact ion pairs (CIPs) (j = 1) and arising from the cooperative H-bond-network rearrangement process (coop., j = 2), and fast H-bond-flip (j = 3) of water.

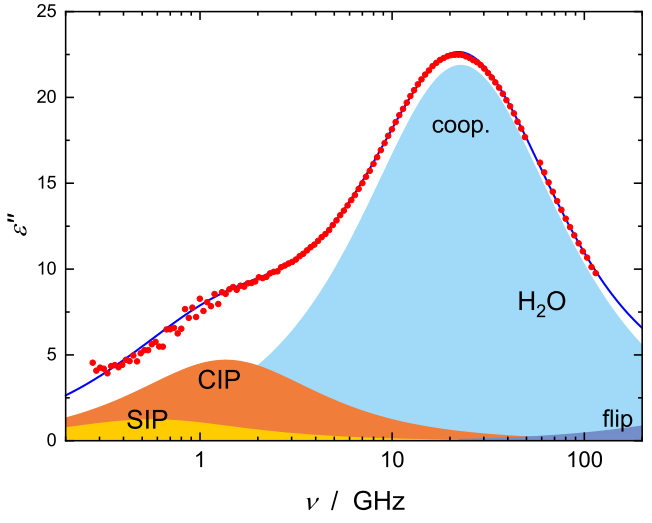

Figure 3. Dielectric loss, $\varepsilon''(\nu)$, spectrum of 1.293 M aqueous solution of $Cd(NO_3)_2$ at 25 °C (symbols) and its fit with the D+D+CC+D model (line). Shaded areas indicate the contributions of solvent-shared ion pairs (SIPs) (j = 1), CIPs (j = 2), and water, arising from its cooperative H-bond-network rearrangement process (coop., j = 3), and fast H-bond-flip (j = 4).

Relaxation amplitudes, S_i, assigned to a particular dipolar species, i (not necessarily identical to a resolved mode, j), were evaluated with

$$S_i = \frac{\varepsilon}{\varepsilon + A_i(1-\varepsilon)} \times \frac{N_A}{3k_B T \epsilon_0} \times c_i \times \mu_{\mathrm{eff},i}^2 \quad (3)$$

In this equation c_i is the dipole concentration, $\mu_{\mathrm{eff},i}$ its effective dipole moment, and A_i the shape-dependent cavity-field factor; N_A, k_B, and ϵ_0 have their usual meanings.[7,12]

RESULTS AND DISCUSSION

Based on the spectrum of neat water,[12,24] the concentration dependence of the peak frequencies/relaxation times (Figure S5) and their amplitudes (Figure 4), the two highest-frequency modes of all four salts can be straightforwardly assigned to the

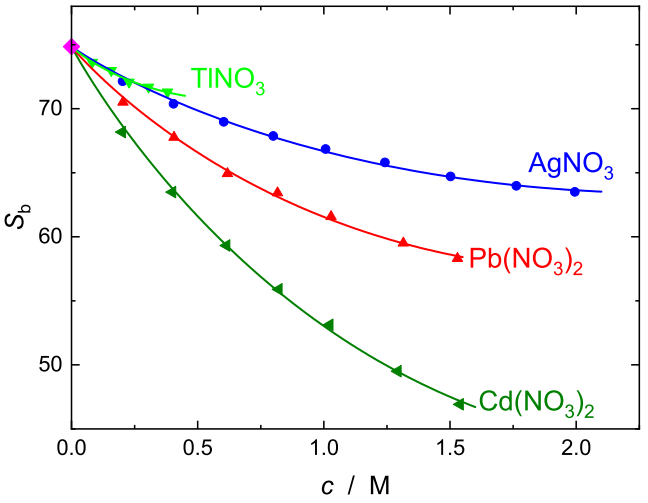

Figure 4. Bulk-water amplitudes, S_b (symbols), and their fits (lines), of aqueous solutions of $AgNO_3$ (blue ○), $TlNO_3$ (green ▽), $Pb(NO_3)_2$ (red △), and $Cd(NO_3)_2$ (olive ◁) solutions as a function of solute concentration, c, at 25 °C. Value for neat water (diamond) taken from Eiberweiser et al.[12]

cooperative rearrangement of the hydrogen-bond network of bulk water (j = 2 in the D+CC+D model; j = 3 in the D+D+CC+D model) and to its preceding fast H-bond flip (D+CC+D: j = 3; D+D+CC+D: j = 4).[22]

Based on the concentration dependence of their amplitudes, the lower-frequency modes in the spectra are clearly solute-related. For $Cd(NO_3)_2$(aq) solutions, judging from their τ_1 values the likely origin of this mode is either ion-cloud relaxation or the reorientation of solvent-shared ion pairs (SIPs). For the other salts, values for τ_1 (as well as τ_2 for $Cd(NO_3)_2$(aq)) suggest contact ion pairs (CIPs) and/or dynamically retarded (slow) hydrating H_2O molecules.[7] Evaluation of the relevant amplitudes ruled out both ion-cloud relaxation and slow water as the sources of these lower-frequency modes. Accordingly, these options were not considered further. Ion-related modes contributing to the solution spectra at $\nu \gtrsim 100$ GHz[23,25−28] are too weak to be resolved with the present experiments and are thus neglected in the data analysis.

Ion Hydration. The fast hydrogen-bond flip of individual H_2O molecules and the subsequent resettlement of the H-bond network of solvent water are connected events.[22] Neglecting possible weak contributions to S_4 from cage-rattling of the ions,[23] the relaxation amplitude of (more-or-less) unperturbed bulk water in these solutions is given by $S_b = S_2 + S_3$ for the D+CC+D model and by $S_b = S_3 + S_4$ for the D+D+CC+D model. As expected from the concentration-dependent electric fields around the ions,[29] all studied salts exhibit a nonlinear decrease of S_b with rising concentration. This decrease becomes larger in the sequence $TlNO_3 \approx AgNO_3 < Pb(NO_3)_2 < Cd(NO_3)_2$ (Figure 4).

The experimental bulk-water amplitude, $S_b(c)$, at salt concentration c, can be written as

$$S_b(c) = S_b^{eq}(c) - \Delta\varepsilon_{kd} \quad (4)$$

In eq 4, $S_b^{eq}(c)$ represents the equilibrium amplitude of the solvent, which is determined by the analytical water concentration, c_w, and by the static (equilibrium) depolarization of the

https://doi.org/10.1021/acs.jpcb.4c05441
J. Phys. Chem. B XXXX, XXX, XXX−XXX

solvent due to the alignment of H_2O dipoles by the electric field of the ions. From $S_b^{eq}(c)$ the concentration of DRS-detected bulk water, c_b, is obtained with eq 3.[7]

The second term in eq 4, $\Delta\varepsilon_{kd}$, describes the additional kinetic depolarization (kd) of solvent dipoles due to ion migration.[30] The magnitude of kd is proportional to the solution conductivity, κ, and can be obtained from the equation of Sega et al.[31]

$$\Delta\varepsilon_{kd} = \Delta\varepsilon_{kd}^{HO}\cdot\exp(\sigma R)\cdot(\sigma R + 2)/2 \quad (5)$$

where

$$\Delta\varepsilon_{kd}^{HO} = p\cdot\frac{\varepsilon(0) - \varepsilon_\infty(0)}{\varepsilon(0)}\cdot\frac{\tau(0)}{\varepsilon_0}\cdot\kappa \quad (6)$$

is the decrement at vanishing salt concentration, given by the corrected continuum model of Hubbard and Onsager (HO),[30] σ is the reciprocal Debye length at a given ionic strength, R is the average effective ion radius, $\varepsilon(0)$ and $\varepsilon_\infty(0)$ are respectively the static and infinite-frequency permittivities of the neat solvent, $\tau(0)$ is the relaxation time of the dominant solvent dispersion step and p is a hydrodynamic parameter that accounts for the coupling of translational ion motions to the macroscopic viscosity.

For the present work, slip boundary conditions ($p = 2/3$) and $R = (r_+ + r_-)/2$ were assumed. The required ion radii, r_j (Table S5) were taken from Marcus.[32] Figure S5 illustrates the impact of kinetic depolarization on the resulting effective hydration numbers (see below). The effective dipole moment of 3.746 D, obtained from the data for neat water, was used when calculating $c_b(c)$ from $S_b^{eq}(c)$ with eq 3.[33]

The thus-obtained effective bulk-water concentrations, c_b, yielded values for the effective total hydration numbers of the salts

$$Z_t = (c_w - c_b)/c \quad (7)$$

as the total number of dynamically retarded H_2O dipoles per equivalent of salt (Figure 5).[7] Note that Z_t reflects the amount of apparently missing bulk water but not how strongly it is affected dynamically, i.e., whether the dipoles are "frozen" (irrotationally bound, ib) on the time scale of the experiment, or just slowed down sufficiently to produce a new lower-frequency relaxation mode in the spectrum. In principle, the lower-frequency modes observed for the present solutions could at least partly arise from such "slow water." However, evaluation of the amplitudes of these processes as a function of solute concentration yielded results that were neither self-consistent nor compatible with previous findings.[7,33,34] Accordingly, the present total hydration numbers were exclusively assigned to irrotationally bound H_2O dipoles, i.e., $Z_t = Z_{ib}$.

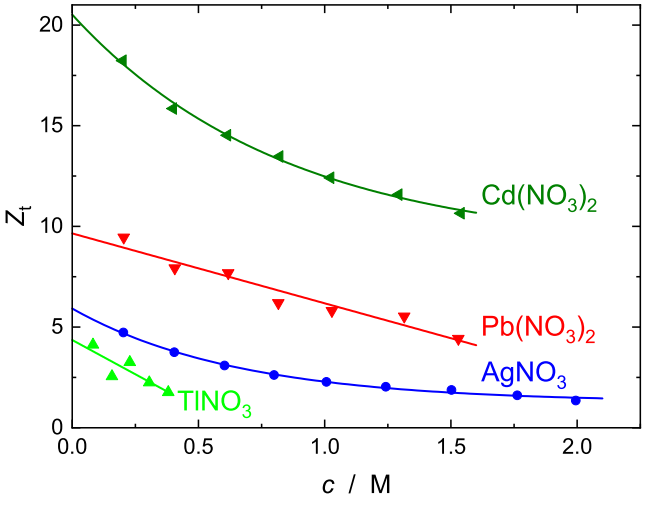

Figure 5. Effective total hydration numbers, Z_t (symbols), and their fits (lines; see Table 1 for details) for aqueous solutions of $AgNO_3$, $TlNO_3$, $Cd(NO_3)_2$, and $Pb(NO_3)_2$ at 25 °C.

Detailed analysis of the DR spectra of simple nitrate salts such as $NaNO_3$ in aqueous solution,[35] as well as information from double-difference-IR spectroscopy,[36] 2D-IR spectroscopy,[37,38] and *ab initio* MD simulations[39] indicate that the nitrate ion does not slow down but accelerates the dynamics of the ~6 to 9 H_2O molecules[40] in its hydration shell. Obviously, the associated relaxation time does not differ sufficiently from that of bulk water to allow resolution of this contribution as a separate mode in the present DR spectra. The increasing amount of this fast hydration water is almost certainly the main reason for the observed decrease of τ_2 with rising c (Figure S6). Similar to the situation for Cl^-,[41] we therefore reasonably assume $Z_t(NO_3^-) = 0$ in the following analysis.

Accordingly, the effective hydration numbers shown in Figure 5 can be assigned fully to the cations. In line with their surface-charge densities, $Z_t(M(NO_3)_z) = Z_{ib}(M(NO_3)_z) = Z_{ib}(M^{z+})$ increases in the order $Tl^+ < Ag^+ < Pb^{2+} < Cd^{2+}$. While the Z_t values for Tl^+ and Pb^{2+} decrease linearly with rising c, those for Ag^+ and Cd^{2+} exhibit an exponential decay, apparently leveling off respectively at $a_1 \approx 1.3$ and ~11.6 at high c, (Table 1).

Table 1. Parameters Z_t^0, a_1, and a_2 Describing the Concentration Dependence of the Effective Total Cation Hydration Numbers, Z_t, of the Studied Metal Nitrates, and First-Shell Cation Coordination Numbers, CN_+, from the Literature[a,b]

	Z_t^0	a_1	a_2	$CN_+^{(1)}$
$TlNO_3$[c]	4.4 ± 0.6		6.8 ± 2.2	5.9[9]
$AgNO_3$[d]	5.9 ± 0.3	1.3 ± 0.1	0.66 ± 0.06	2 + 3 and 2 + 4;[43] 2 + x[44]
$Pb(NO_3)_2$[c]	9.7 ± 0.4		3.5 ± 0.4	8.1;[45] 6;[11] 6–9[46]
$Cd(NO_3)_2$[d]	20.5 ± 1.2	11.6 ± 0.5	0.85 ± 0.13	6–7[10,40,47]

[a]Based on the assumption $Z_t(NO_3^-) = 0$, see text for details. [b]Units: a_2 in M^{-1}. [c]$Z_t = Z_t^0 - a_2 \times c$. [d]$Z_t = a_1 + (Z_t^0 - a_1) \times \exp(-c/a_2)$.

However, for none of the present salts does the concentration dependence of $Z_t(c)$ exhibit a discontinuity at the concentration where (due to crowding) the anion starts to penetrate the second hydration shell of the cation (Ag^+: ~1.29 M; Tl^+: ~1.14 M; Cd^{2+}: ~0.92 M; Pb^{2+}: ~0.85 M).[42]

Ion−ion interactions, which can lead to a "softening" or breakup of ion hydration shells, are negligible as $c \to 0$. Accordingly, the intercepts $Z_t^0(M^{z+})$ reflect the strength of cation-water interactions. For those, the electrostatic force between cation charge and H_2O dipole moment, and thus the surface-charge density of the ion, $z_+e_0/(4\pi r_+^2)$ (e_0 is the elementary charge), is commonly assumed to be the dominant factor.[52] Figure 6 shows that $Z_t^0(M^{z+})$ indeed correlates reasonably with cation surface-charge density, although increasing deviations at high Z_t^0 and/or $z_+e_0/(4\pi r_+^2)$ values are obvious.

https://doi.org/10.1021/acs.jpcb.4c05441
J. Phys. Chem. B XXXX, XXX, XXX−XXX

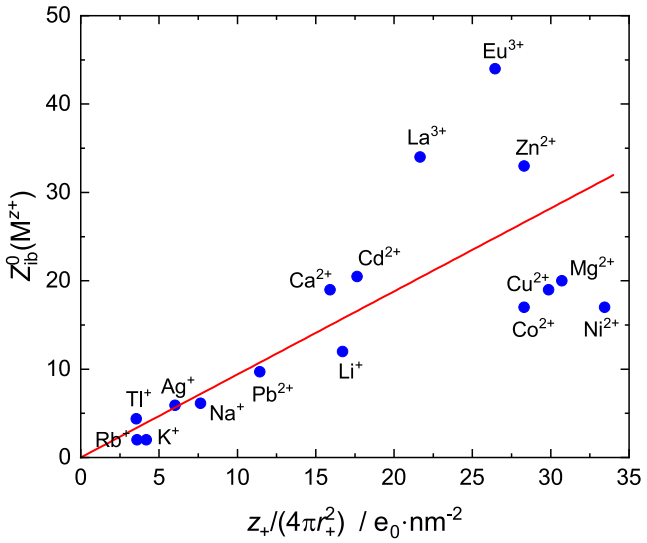

Figure 6. Number, $Z^0_{ib}(M^{z+})$, of H_2O dipoles frozen (irrotationally bound) by the cation at $c \to 0$ as a function of its surface-charge density, $z_+e_0/(4\pi r_+^2)$ (e_0 is the elementary charge), for the present cations and literature data.[33,41,48−51] Note that $Z^0_{ib}(M^{z+}) = Z^0_t(M^{z+})$, except for K^+ and Rb^+, where $Z^0_{ib} < Z^0_t$.[41] The line is a linear fit of all data forced through the origin.

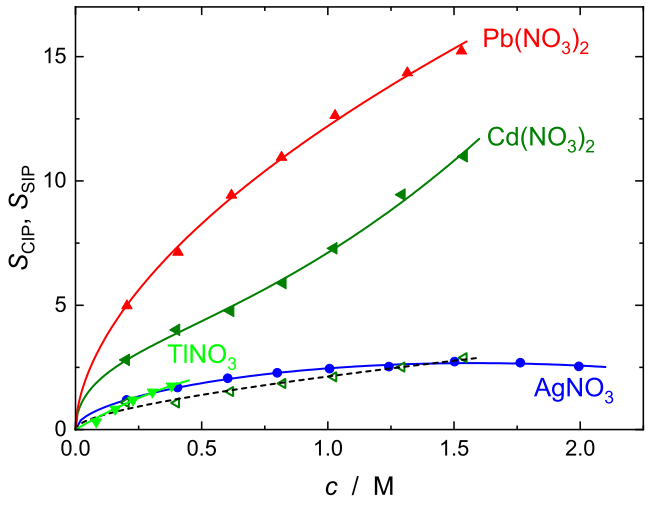

Figure 7. Contact-ion-pair amplitudes, S_{CIP} (filled symbols), and their fits (solid lines), for aqueous solutions of: $AgNO_3$ (blue ○), $TlNO_3$ (green ▽), $Cd(NO_3)_2$ (olive ◁), and $Pb(NO_3)_2$ (red △) as functions of solute concentration, c, at 25 °C. Also included is the amplitude, S_{SIP} (open symbols, broken line), assigned to solvent-shared $[Cd(OH_2)NO_3]^+$(aq) ion pairs.

The intercepts $Z^0_t(M^{z+})$ can also be compared with cation coordination numbers, CN_+, derived from computer simulations or scattering experiments.[7] Generally, such data are only available for the first hydration shell ($CN^{(1)}_+$) but in some cases also the number of second-nearest neighbors, $CN^{(2)}_+$, was determined.[40] According to the data for Ag^+[43,44] and Pb^{2+},[11,45,46] $Z^0_t \approx CN^{(1)}_+$ (Table 1). This means that the dynamics of the H_2O molecules residing in the second hydration shell of these ions (~5 to 17[8,40] for Ag^+ and ~12[11] for Pb^{2+}) are too similar to bulk water to be resolved by DRS. In contrast, H_2O dipoles in direct contact with Tl^+ are apparently not completely frozen (Table 1), in line with results from QM/MM-MD simulations,[9] revealing a somewhat dynamic hydration shell for this ion. In dilute aqueous solutions the first hydration shell of Cd^{2+} contains 6−7 H_2O molecules[10,40,47] whereas ~14 to 16 H_2O molecules are in the second shell.[10] Thus, the present value of $Z^0_t(Cd^{2+}) = 20.5 \pm 1.2$ (Table 1) indicates that as $c \to 0$ the water dipoles in the second hydration shell become essentially frozen. As c increases, $Z_t \to 11.6 > CN^{(1)}_+$. This suggests that the marked nonlinear decrease of $Z_t(c)$ with increasing c for Cd^{2+}(aq) (Figure 5) mainly reflects second-hydration shell breakup due to ion−ion interactions, similar to results reported for other divalent cations such as Mg^{2+}, Ca^{2+}, Cu^{2+}, Co^{2+} or Ni^{2+}.[33,48,49] For Ag^+(aq) one may speculate that the drop of $Z_t(c)$ from $Z^0_t \approx 5.9$ to ~1.3 reflects the unusual solvation shell structure of this ion: a well-defined (thus long-lived) linear $[Ag(H_2O)_2]^+$ moiety with a few more mobile perpendicular H_2O dipoles at slightly longer Ag−O distances.[44]

The influence of the dissolved ions is not restricted to their immediate hydration shell(s) but also affects bulk-water dynamics. For the present salts the relaxation time associated with the cooperative resettling of the H-bond network, τ_{CC} ($=\tau_2$ for the D+CC+D model; $=\tau_3$ for the D+D+CC+D model), exhibits a significant initial decrease with increasing c before leveling at $c \gtrsim 0.7$ M (Figure S6). Simultaneously, the associated peak-width parameter, α_{CC}, rises monotonically (Figure 7), indicating increasing microheterogeneity of the solvent molecules in the solutions. The increasing concentration of nitrate ions is one reason for the drop of $\tau_{CC}(c)$, because the orientational relaxation time of H_2O molecules in the immediate vicinity of the anion reaches only ~60% of the bulk water value.[39] However, the cations also have an effect since the decrease of $\tau_{CC}(c)$ follows the surface-charge density of the cation (Figure S6). This may indicate an increasing mismatch between the structures of bulk- and hydration-shell water, reducing the number of H-bonds between them. Indeed, for all studied cations simulations suggest rather mobile second hydration shells with frequent exchange of H_2O molecules with the bulk.[9,44,45,47] Also, results from DRS,[53,54] Raman,[54] and terahertz spectroscopy[28] suggest the existence of such a region of hypermobile water around many ions.

Solute Relaxation(s). All the present electrolytes exhibited a low-frequency mode centered at ~1.5 to 3.0 GHz (Figures 2 and 3). From the corresponding relaxation times of ca. ~50 to 100 ps (Tables S1−S4) the most plausible origins of this mode are either dynamically retarded (but not frozen) cation hydration-shell water or the formation of contact ion pairs (CIPs). As indicated in the previous section, the amplitudes of this mode (Figure 7) yielded "slow water" hydration numbers, Z_s, greater than the total amount of bound water, Z_t (Figure 5), which is physically impossible. On the other hand, there is convincing evidence in the literature that all four cations form weak (or very weak) ion pairs with nitrate in aqueous solution.[55−62] Accordingly, and consistent with its location in the spectra, this relaxation mode is attributed to CIPs for $AgNO_3$, $TlNO_3$, $Cd(NO_3)_2$ and $Pb(NO_3)_2$. The additional lowest-frequency mode resolved for the cadmium salt centered at ~0.6 GHz (Figure 3) is assigned to solvent-shared ion pairs (SIPs), $[Cd(OH_2)NO_3]^+$(aq), in line with the strong hydration of Cd^{2+} (see above).

Effective ion-pair dipole moments, $\mu_{eff,IP} = \mu_{IP}/(1 - f_{IP}\alpha_{IP})$, reaction-field, f_{IP}, and cavity-field factors, A_{IP}, required to calculate ion-pair concentrations, c_{IP}, via eq 3 using the ion-pair amplitudes, S_{CIP} and S_{SIP} of Figure 7, were obtained following the procedure of Barthel et al.[63] Radii, r_i, and electronic polarizabilities, α_i, of cations ($i = +$), anions ($-$) and solvent (w) are summarized in Table S5.[32] The polarizability of the ion pair

https://doi.org/10.1021/acs.jpcb.4c05441
J. Phys. Chem. B XXXX, XXX, XXX−XXX

Table 2. Ion-Pair Dipole Moments, μ_{IP}; Parameters K_i^0 (i = A or SIP), B, and C of eq 9 or K_{CIP}^0 and B for the Linear Fit of K_{CIP}; and K_A^0 Values from the Literature[a]

	IP	μ_{IP}	K_A^0	B	C	K_A^0(lit)
$AgNO_3$	CIP	12.58	4.6 ± 0.7	−2.26 ± 0.23	0.98 ± 0.15	3.7[b]
$TlNO_3$	CIP	13.81	2.38 ± 0.13	−1.40 ± 0.09		2.3,[b] 3.2[56]
$Pb(NO_3)_2$	CIP	18.96	6.6 ± 0.9	−0.62 ± 0.08	0.18 ± 0.03	see text
$Cd(NO_3)_2$	SIP+CIP		8.7 ± 2.8[c]	−0.84 ± 0.03	0.28 ± 0.02	see text
	SIP	45.69	0.76 ± 0.23	−0.87 ± 0.18	0.29 ± 0.08	
	CIP	20.30	10.4 ± 1.1	0.8 ± 0.4[d]		

[a]Units: μ_{IP} in D; K_A^0, K_{SIP}^0, K_A^0(lit) in M^{-1}; B in M^{-1}; C in $M^{-3/2}$. [b]Values of Tsierkezos and Ritter[61] interpolated to 298.15 K. [c]Fixed to $K_A^0 = K_{SIP}^0 + K_{SIP}^0 K_{CIP}^0$. [d]Linear fit $K_{SIP} = K_{SIP}^0 + B \times I$.

α_{IP} was estimated as $\alpha_+ + \alpha_- + m\alpha_w$, with $m = 0$ for CIPs and 1 for SIPs. The center of hydrodynamic stress was taken to be the pivot for the charged $[PbNO_3]^+(aq)$ and $[Cd(OH_2)_mNO_3]^+(aq)$ ion pairs.[64] The resulting permanent (vacuum) ion-pair dipole moments, μ_{IP}, are included in Table 2.

Overall association constants, $K_A = c_{IP}/(c_+c_-)$, calculated from the total ion-pair concentrations, c_{IP}, for $TlNO_3(aq)$, $AgNO_3(aq)$, and $Pb(NO_3)_2(aq)$, where only CIPs were detected, are shown as a function of ionic strength in Figure 8.

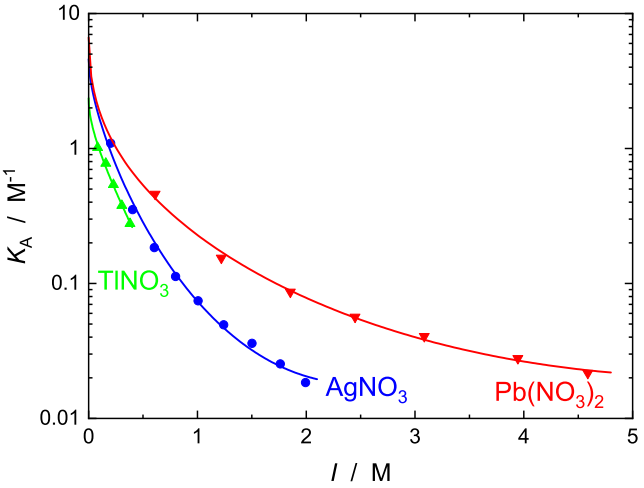

Figure 8. Association constants, K_A (symbols), for aqueous solutions of $AgNO_3$, $TlNO_3$, and $Pb(NO_3)_2$ as a function of ionic strength, I, at 25 °C, assuming only CIP formation. Lines are fits with eq 9 (see Table 2).

Note that under these conditions $c_{IP} = c_{CIP}$, $c_+ = c - c_{IP}$ and $c_- = \nu_- c - c_{IP}$ (where $\nu_- = 1$ or 2 is the stoichiometric coefficient of the anion). The equivalent data for $Cd(NO_3)_2(aq)$, where $c_{IP} = c_{CIP} + c_{SIP}$, as well as the stepwise association constants, $K_{SIP} = c_{SIP}/(c_+c_-)$ and $K_{CIP} = c_{CIP}/c_{SIP}$, corresponding to the equilibria

$$\underset{\text{freeions}}{Cd^{2+}(aq) + NO_3^-(aq)} \overset{K_{SIP}}{\rightleftharpoons} \underset{\text{SIP}}{[Cd(OH_2)NO_3]^+(aq)}$$

$$\underset{\text{SIP}}{[Cd(OH_2NO_3]^+(aq)} \overset{K_{CIP}}{\rightleftharpoons} \underset{\text{CIP}}{[CdNO_3]^+(aq)} \quad (8)$$

are shown in Figure 9.

For all four studied electrolytes, K_A values show the typical decrease with rising nominal ionic strength, $I = 0.5 \times \sum c_i z_i^2$ (i = +, −), that can be described for convenience by an extended Guggenheim-type equation[34,65]

$$\log K_A = \log K_A^0 - \frac{2A_{DH}|z_+z_-|\sqrt{I}}{1+\sqrt{I}} + B{\cdot}I + C{\cdot}I^{3/2} \quad (9)$$

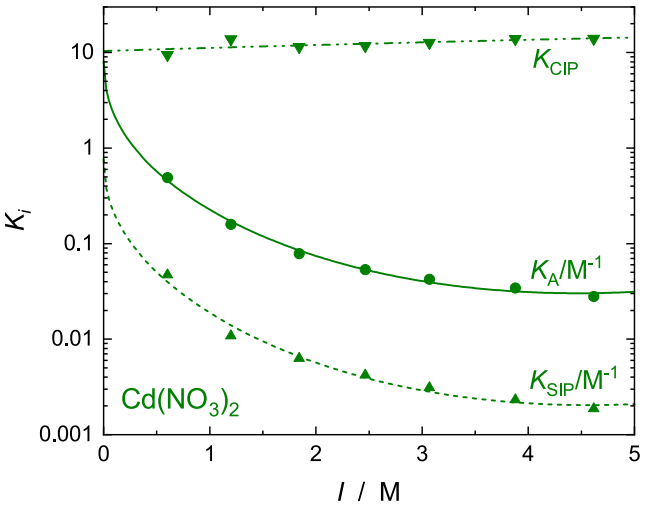

Figure 9. Overall K_A (●), and stepwise association constants for SIP, K_{SIP} (▲), and for CIP, K_{CIP} (▼), in aqueous solutions of $Cd(NO_3)_2$ as a function of ionic strength, I, at 25 °C. Lines are fits with eq 9 for K_A and K_{SIP}, or a linear fit for K_{CIP} (see data in Table 2).

where K_A^0 is the standard state (infinite dilution) association constant, z_+ and z_- are the ion charge numbers, $A_{DH} = 0.5115(L\ mol^{-1})^{1/2}$ is the Debye−Hückel constant for activity coefficients in water at 25 °C, and B and C are adjustable parameters. Equation 9 also describes the ionic-strength dependence of K_{SIP} for $Cd(NO_3)_2(aq)$, whereas $\log K_{CIP}$ exhibits a weak linear increase (Figure 9). The corresponding fit parameters are summarized in Table 2.

All the present nitrate salts exhibit weak to very weak ion association, with K_A values at any given ionic strength (including infinite dilution, Table 2), following the order $Tl^+ < Ag^+ < Pb^{2+} < Cd^{2+}$ (Figures 8 and 9) consistent with the charge/radius ratio of the cations. Perhaps more significantly, given that the association reaction involves the replacement of one or more water molecules in the hydration shell(s) of the cation by the incoming NO_3^- ion, the above sequence is also consistent with their (absolute) hydration energies ($-\Delta_{hyd}G° = 310$, 440, 1434, and 1736 kJ·mol^{-1}, respectively).[32]

The K_A^0 values obtained via eq 9 can be compared directly with literature results. For convenience, comparisons with the present results are made with constants taken from the comprehensive IUPAC compilations,[66−68] supplemented where appropriate with more recent publications. However, before attempting such comparisons, some words of warning are appropriate. In general, the reliable measurement of ion-association constants for which $K_A^0 \lesssim 5$ (or even $\lesssim 10$) M^{-1} is extraordinarily difficult (some would say impossible). Some techniques are undoubtedly better than others for the quantification of weak complexes and it is

https://doi.org/10.1021/acs.jpcb.4c05441
J. Phys. Chem. B XXXX, XXX, XXX−XXX

sometimes possible to create favorable circumstances for their measurement.[69,70] Nevertheless, overall the generalization remains valid and it is wise to view all small values of K_A with caution. This unhappy situation is apparent from the rather large uncertainties in the present K_A^0 values, and from the lack of agreement among the literature results, even when no particular problem can be identified.

Despite the concerns just expressed, the agreement between the present and selected literature values of K_A^0 for $AgNO_3^0(aq)$ and $TlNO_3^0(aq)$ is excellent (Table 2). Note, however, that there are other plausible literature results[66−68] that are more scattered.

The situation regarding the formation of $PbNO_3^+(aq)$ is less satisfactory. Several older but apparently reliable investigations using traditional techniques are in good agreement with each other and suggest $K_A^0 \approx 14\ M^{-1}$. However, others cluster around $K_A^0 \approx 3\ M^{-1}$.[66−68] More recent results using ^{207}Pb-NMR[62,71] are lower still but are almost certainly incorrect.[72] On the other hand, Raman spectroscopy appears to tell a different story.[60] Thus, although Xu et al. did not derive equilibrium constants,[60] the CIP concentrations that can be abstracted from their spectra at $c \geq 1$ M are about five-times greater than the present results under comparable conditions. Apart from the different time-scales of Raman and DR spectroscopies, with the former being sensitive to short-lived (<ps) ion contacts while the latter requires an IP lifetime comparable to τ_{CIP}, there is no obvious explanation of these discrepancies. One possibility might be the formation of pseudolinear ion triplets, $[O_3N\ Pb\ NO_3]^0(aq)$, analogous to those found for $M(ClO_4)_2$ in acetonitrile.[73] Such species are Raman-active but do not have a DRS signature. All that can be said is that the present result: $K_A^0 \approx 7\ M^{-1}$ (Table 2) sits in the middle of these disparate values.

The formation constant for $CdNO_3^+(aq)$ has been less well reported in the literature. Based on the systematic behavior noted above, the present DRS results: $K_A^0(CdNO_3^+) > K_A^0(PbNO_3^+)$ would seem to be more realistic than the opposite suggested by the sparse and uncertain literature values.[66−68]

As noted in the Introduction, a great advantage of DRS is its ability to identify and quantify the types of ion pairs present, i.e., the extent to which they exist as CIPs, SIPs or 2SIPs.[7] The DR spectra for the nitrate solutions of Ag^+, Tl^+ and Pb^{2+} identify, from their location in the frequency domain, the presence only of CIPs. For the more strongly hydrated Cd^{2+}, SIPs are also formed (albeit in only small amounts). In this context it is interesting to note that ^{207}Pb-NMR spectra[62,71] also indicate the presence of CIPs in $Pb(NO_3)_2(aq)$ solutions. Raman measurements[60,74] on various divalent nitrate solutions show that stronger cation hydration results in increasing formation of SIPs, as found here for $Cd(NO_3)_2(aq)$ solutions.

CONCLUSIONS

Broadband dielectric relaxation spectra of the aqueous solutions of four heavy-metal nitrate salts ($TlNO_3$, $AgNO_3$, $Pb(NO_3)_2$ and $Cd(NO_3)_2$) at 25 °C reveal the presence of three or (for the Cd salt only) four modes: one (two for Cd) solute-related mode(s) at lower frequencies and two solvent-related modes at higher frequencies. Detailed analysis of the latter indicated that all four cations were strongly hydrated with effective hydration numbers (Z_t values) of approximately 4, 6, 10, and 20 irrotationally bound water molecules at infinite dilution for Tl^+, Ag^+, Pb^{2+} and Cd^{2+}, respectively, consistent with the partial retardation of H_2O molecules in the second hydration shell for $Pb^{2+}(aq)$ and especially for $Cd^{2+}(aq)$. The solute-related mode(s) were consistent with the rotational diffusion of contact ion pairs in all four systems, with small amounts of solvent-shared IPs for the more strongly hydrated $Cd^{2+}(aq)$. The present overall ion-pair formation constants are in good agreement with literature values for $TlNO_3^0(aq)$ and $AgNO_3^0(aq)$. However, the agreement is less satisfactory for $PbNO_3^+(aq)$ and $CdNO_3^+(aq)$. Such differences are at least partly due to inadequacies in the literature data. There is a clear need for careful redetermination of these constants using reliable techniques such as metal amalgam potentiometry.

ASSOCIATED CONTENT

Supporting Information

The Supporting Information is available free of charge at https://pubs.acs.org/doi/10.1021/acs.jpcb.4c05441.

Tables with experimental densities, conductivities and dielectric relaxation parameters of the investigated solutions; additional figures supporting data processing and discussion (PDF)

AUTHOR INFORMATION

Corresponding Authors

Johannes Hunger − *Department for Molecular Spectroscopy, Max Planck Institute for Polymer Research, D-55128 Mainz, Germany*; orcid.org/0000-0002-4419-5220; Email: hunger@mpip-mainz.mpg.de

Richard Buchner − *Institut für Physikalische und Theoretische Chemie, Universität Regensburg, D-93040 Regensburg, Germany*; orcid.org/0000-0003-3029-1278; Email: richard.buchner@chemie.uni-regensburg.de

Glenn Hefter − *Chemistry Department, Murdoch University, Murdoch, WA 6150, Australia*; orcid.org/0000-0001-9388-2783; Email: g.hefter@murdoch.edu.au

Complete contact information is available at: https://pubs.acs.org/10.1021/acs.jpcb.4c05441

Notes

The authors declare no competing financial interest.

ACKNOWLEDGMENTS

The authors thank Ms Martina Knecht for recording the DRS data. J.H. acknowledges funding from the Max Planck Society.; G.H. and R.B. had no financial support.

REFERENCES

(1) Burgess, J. *Metal Ions in Solution*; Ellis Horwood: Chichester, UK, 1978.

(2) Burkin, A. R., Ed. *Chemical Hydrometallurgy: Theory and Principles*; Imperial College Press: London, UK, 2001.

(3) Marcus, Y.; Hefter, G. Ion Pairing. *Chem. Rev.* **2006**, *106*, 4585−4621.

(4) Marcus, Y. *Ions in Solution and Their Solvation*; John Wiley: Hoboken, USA, 2015.

(5) Briffa, J.; Sinagra, E.; Blundell, R. Heavy Metal Pollution in the Environment and their Toxicological Effects on Humans. *Heliyon* **2020**, *6*, e04691.

(6) Jadaa, W.; Mohammed, H. K. Heavy Metals - Definition, Natural and Anthropogenic Sources of Releasing into Ecosystems, Toxicity, and Removal Methods - An Overview Study. *J. Ecol. Eng.* **2023**, *24*, 249−271.

(7) Buchner, R.; Hefter, G. Interactions and Dynamics in Electrolyte Solutions by Dielectric Spectroscopy. *Phys. Chem. Chem. Phys.* **2009**, *11*, 8984−8999.

(8) Persson, I.; Nilsson, K. B. Coordination Chemistry of the Solvated Silver(I) Ion in the Oxygen Donor Solvents Water, Dimethyl Sulfoxide, and N,N′-Dimethylpropyleneurea. *Inorg. Chem.* **2006**, *45*, 7428−7434.
(9) Vchirawongkwin, V.; Hofer, T. S.; Randolf, B. R.; Rode, B. M. Tl(I)-The Strongest Structure-Breaking Metal Ion in Water? A Quantum Mechanical/Molecular Mechanical Simulation Study. *J. Comput. Chem.* **2007**, *28*, 1006−1016.
(10) Smirnov, P. R. Structural Parameters of the Nearest Environment of Zinc, Cadmium, and Mercury Ions in Aqueous Solutions of Their Salts (A Review). *Russ. J. Gen. Chem.* **2024**, *94*, 145−153.
(11) Persson, I.; Lyczko, K.; Lundberg, D.; Eriksson, L.; Płaczek, A. Coordination Chemistry Study of Hydrated and Solvated Lead(II) Ions in Solution and Solid State. *Inorg. Chem.* **2011**, *50*, 1058−1072.
(12) Eiberweiser, A.; Nazet, A.; Hefter, G.; Buchner, R. Ion Hydration and Association in Aqueous Potassium Phosphate Solutions. *J. Phys. Chem. B* **2015**, *119*, 5270−5281.
(13) Lide, D. R., Ed. *CRC Handbook of Chemistry and Physics*, 84th ed.; CRC Press: Boca Raton, USA, 2004.
(14) Blackham, D. V.; Pollard, R. D. An Improved Technique for Permittivity Measurements Using a Coaxial Probe. *IEEE Trans. Instrum. Meas.* **1997**, *46*, 1093−1099.
(15) Kaatze, U. Measuring the Dielectric Properties of Materials. Ninety-year Development from Low-frequency Techniques to Broadband Spectroscopy and High-frequency Imaging. *Meas. Sci. Technol.* **2013**, *24*, 012005.
(16) Ensing, W.; Hunger, J.; Ottoson, N.; Bakker, H. J. On the Orientational Mobility of Water Molecules in Proton and Sodium Terminated Nafion Membranes. *J. Phys. Chem. C* **2013**, *117*, 12930−12935.
(17) Böttcher, C. F. J.; Bordewijk, P. *Theory of Electric Polarization*; Elsevier: Amsterdam, 1978; Vol. 2.
(18) Kremer, F.; Schönhals, A., Eds. *Broadband Dielectric Spectroscopy*; Springer: Berlin, Germany, 2003.
(19) Balos, V.; Kim, H.; Bonn, M.; Hunger, J. Dissecting Hofmeister Effects: Direct Anion-Amide Interactions Are Weaker than Cation-Amide Binding. *Angew. Chem., Int. Ed.* **2016**, *55*, 8125−8128.
(20) Schrödle, S.; Hefter, G.; Kunz, W.; Buchner, R. Effects of the Non-ionic Surfactant $C_{12}E_5$ on the Cooperative Dynamics of Water. *Langmuir* **2006**, *22*, 924−932.
(21) Stoppa, A.; Nazet, A.; Buchner, R.; Thoman, A.; Walther, M. Dielectric Response and Collective Dynamics of Acetonitrile. *J. Mol. Liq.* **2015**, *212*, 963−968.
(22) Laage, D.; Stirnemann, G.; Sterpone, F.; Rey, R.; Hynes, J. T. Reorientation and Allied Dynamics in Water and Aqueous Solutions. *Annu. Rev. Phys. Chem.* **2011**, *62*, 395−416.
(23) Balos, V.; Imoto, S.; Netz, R. R.; Bonn, M.; Bonthuis, D. J.; Nagata, Y.; Hunger, J. Macroscopic Conductivity of Aqueous Electrolyte Solutions Scales with Ultrafast Microscopic Ion Motions. *Nat. Commun.* **2020**, *11*, No. 1611.
(24) Fukasawa, T.; Sato, T.; Watanabe, J.; Hama, Y.; Kunz, W.; Buchner, R. The Relation between Dielectric and Low-frequency Raman Spectra of Hydrogen-bond Liquids. *Phys. Rev. Lett.* **2005**, *95*, 197802.
(25) Schröder, C.; Hunger, J.; Stoppa, A.; Buchner, R.; Steinhauser, O. On the Collective Network of Ionic Liquid/Water Mixtures. II. Decomposition and Interpretation of Dielectric Spectra. *J. Chem. Phys.* **2008**, *129*, 184501.
(26) Song, X. Solvation Dynamics in Ionic Fluids: An Extended Debye-Hückel Dielectric Continuum Model. *J. Chem. Phys.* **2009**, *131*, 044503.
(27) Rinne, K. F.; Gekle, S.; Netz, R. R. Dissecting Ion-specific Dielectric Spectra of Sodium-halide Solutions into Solvation Water and Ionic Contributions. *J. Chem. Phys.* **2014**, *141*, 214502.
(28) Singh, A. K.; Doan, L. C.; Lou, D.; Wen, C.; Vinh, N. Q. Interfacial Layers between Ion and Water Detected by Terahertz Spectroscopy. *J. Chem. Phys.* **2022**, *157*, 054501.
(29) Gavish, N.; Promislow, K. Dependence of the dielectric constant of electrolyte solutions on ionic concentration: A microfield approach. *Phys. Rev. E* **2016**, *94*, 012611.
(30) Hubbard, J. B.; Colonomos, P.; Wolynes, P. G. Molecular Theory of Solvated Ion Dynamics. III. The Kinetic Dielectric Decrement. *J. Chem. Phys.* **1979**, *71*, 2652−2661.
(31) Sega, M.; Kantorovich, S.; Arnold, A. Kinetic Dielectric Decrement Revisited: Phenomenology of Finite Ion Concentrations. *Phys. Chem. Chem. Phys.* **2015**, *17*, 130−133.
(32) Marcus, Y. *Ion Properties*; CRC Press: Boca Raton, USA, 1997.
(33) Friesen, S.; Hefter, G.; Buchner, R. Cation Hydration and Ion Pairing in Aqueous Solutions of $MgCl_2$ and $CaCl_2$. *J. Phys. Chem. B* **2019**, *123*, 891−900.
(34) Buchner, R. What can be learnt from Dielectric Relaxation Spectroscopy about Ion Solvation and Association? *Pure Appl. Chem.* **2008**, *80*, 1239−1252.
(35) Wachter, W.; Kunz, W.; Buchner, R.; Hefter, G. Is there a Hofmeister Effect on Water Dynamics? Dielectric Spectroscopy of Aqueous Solutions of NaBr, NaI, $NaNO_3$, $NaClO_4$ and NaSCN. *J. Phys. Chem. A* **2005**, *109*, 8675−8683.
(36) Stangret, J.; Gampe, T. Ionic Hydration Behaviour Derived From Infrared Spectra in HDO. *J. Phys. Chem. A* **2002**, *106*, 5393−5402.
(37) Thøgersen, J.; Réhault, J.; Odelius, M.; Ogden, T.; Jena, N. K.; Jensen, S. J. K.; Keiding, S. R.; Helbing, J. Hydration Dynamics of Aqueous Nitrate. *J. Phys. Chem. B* **2013**, *117*, 3376−3388.
(38) Fournier, J. A.; Carpenter, W.; De Marco, L.; Tokmakoff, A. Interplay of Ion-Water and Water-Water Interactions within the Hydration Shells of Nitrate and Carbonate Directly Probed with 2D IR Spectroscopy. *J. Am. Chem. Soc.* **2016**, *138*, 9634−9645.
(39) Yadav, S.; Choudhary, A.; Chandra, A. A First-Principles Molecular Dynamics Study of the Solvation Shell Structure, Vibrational Spectra, Polarity, and Dynamics around a Nitrate Ion in Aqueous Solution. *J. Phys. Chem. B* **2017**, *121*, 9032−9044.
(40) Ohtaki, H.; Radnai, T. Structure and Dynamics of Hydrated Ions. *Chem. Rev.* **1993**, *93*, 1157−1204.
(41) Buchner, R.; Wachter, W.; Hefter, G. Systematic Variations of Ion Hydration in Aqueous Alkali Metal Fluoride Solutions. *J. Phys. Chem. B* **2019**, *123*, 10868−10876.
(42) Marcus, Y. On Water Structure in Concentrated Salt Solutions. *J. Solution Chem.* **2009**, *38*, 513−516.
(43) Fulton, J. L.; Kathmann, S. M.; Schenter, G. K.; Balasubramanian, M. Hydrated Structure of Ag(I) Ion from Symmetry-Dependent, K- and L-Edge XAFS Multiple Scattering and Molecular Dynamics Simulations. *J. Phys. Chem. A* **2009**, *113*, 13976−13984.
(44) Busato, M.; Melchior, A.; Migliorati, V.; Colella, A.; Persson, I.; Mancini, G.; Veclani, D.; D'Angelo, P. Elusive Coordination of the Ag^+ Ion in Aqueous Solution: Evidence for a Linear Structure. *Inorg. Chem.* **2020**, *59*, 17291−17302.
(45) Bhattacharjee, A.; Hofer, T. S.; Pribil, A. B.; Randolf, B. R.; Lim, L. H. V.; Lichtenberger, A. F.; Rode, B. M. Revisiting the Hydration of Pb(II): a QMCF MD Approach. *J. Phys. Chem. B* **2009**, *113*, 13007−13013.
(46) Kuznetsov, A. M.; Masliy, A. N.; Korshin, G. V. Quantum-chemical Simulations of the Hydration of Pb(II) Ion: Structure, Hydration Energies, and pK_{a1} Value. *J. Mol. Model.* **2018**, *24*, 193.
(47) D'Angelo, P.; Migliorati, V.; Mancini, G.; Cillemi, G.; Barone, V.; Mancini, M.; Sanna, N.; Persson, I. A Coupled Molecular Dynamics and XANES Data Analysis Investigation of Aqueous Cadmium(II). *J. Phys. Chem. A* **2008**, *112*, 11833−11841.
(48) Akilan, C.; Hefter, G. T.; Rohman, N.; Buchner, R. Ion Association and Hydration in Aqueous Solutions of Copper(II) Sulfate from 5°C to 65°C by Dielectric Spectroscopy. *J. Phys. Chem. B* **2006**, *110*, 14961−14970.
(49) Chen, T.; Hefter, G.; Buchner, R. Ion Association and Hydration in Aqueous Solutions of Nickel(II) and Cobalt(II) Sulfate. *J. Solution Chem.* **2005**, *34*, 1045−1066.
(50) Friesen, S.; Krickl, S.; Luger, M.; Nazet, A.; Hefter, G.; Buchner, R. Hydration and Ion Association of La^{3+} and Eu^{3+} in Aqueous Solution. *Phys. Chem. Chem. Phys.* **2018**, *20*, 8812−8821.
(51) Buchner, R.; Hefter, G. Ion Hydration and Association in Aqueous Solutions of Zinc Sulfate by Dielectric Spectroscopy. *J. Mol. Liq.* **2023**, *383*, 122146.

https://doi.org/10.1021/acs.jpcb.4c05441
J. Phys. Chem. B XXXX, XXX, XXX−XXX

(52) Bockris, J. O.; Reddy, A. K. N. *Modern Electrochemistry*, 2nd ed.; Plenum: New York, 1998; Vol. *1*.
(53) Mogami, G.; Miyazaki, T.; Wazawa, T.; Matubayashi, N.; Suzuki, M. Anion-Dependence of Fast Relaxation Component in Na-, K-Halide Solutions at Low Concentrations Measured by High-Resolution Microwave Dielectric Spectroscopy. *J. Phys. Chem. A* **2013**, *117*, 4851−4862.
(54) Okazaki, Y.; Taniuchi, T.; Mogami, G.; Matubayashi, N.; Suzuki, M. Comparative Study on the Properties of Hydration Water of Na- and K-Halide Ions by Raman OH/OD-stretching Spectroscopy and Dielectric Relaxation Data. *J. Phys. Chem. A* **2014**, *118*, 2922−2930.
(55) Nancollas, G. H. Thermodynamics of Ion Association. Part I. Lead Chloride, Bromide, and Nitrate. *J. Chem. Soc.* **1955**, 1458−1462.
(56) D'Aprano, A.; Fuoss, R. M. Conductance of Thallous Nitrate in Dioxane-Water Mixtures at 25°. *J. Phys. Chem. A* **1968**, *78*, 4710−4713.
(57) Irish, D. E.; Davis, A. R.; Plane, R. A. Types of Interaction in Some Aqueous Metal Nitrate Systems. *J. Chem. Phys.* **1969**, *50*, 2262−2263.
(58) Smith, R. M.; Martell, A. E. *Critical Stability Constants: Inorganic Complexes*; Plenum Press: New York, 1976; Vol. *4*.
(59) Caminiti, R.; Cucca, P.; Radnai, T. Investigation on the Structure of Cadmium Nitrate Aqueous Solutions by X-ray Diffraction and Raman Spectroscopy. *J. Phys. Chem. A* **1984**, *88*, 2382−2386.
(60) Xu, M.; Larentzos, J. P.; Roshdy, M.; Criscenti, L. J.; Allen, H. C. Aqueous Divalent Metal-Nitrate Interactions: Hydration versus Ion Pairing. *Phys. Chem. Chem. Phys.* **2008**, *10*, 4793−4801.
(61) Tsierkezos, N. G.; Ritter, U. Thermodynamic Studies on Silver and Thallium Nitrate. *Int. J. Thermophys.* **2011**, *32*, 1950−1965.
(62) Alkan, F.; Small, T.; Bai, S.; Dominowski, A.; Dybowski, C. Ion Pairing in H_2O and D_2O Solutions of Lead Nitrate, as Determined With ^{207}Pb NMR Spectroscopy. *J. Struct. Chem.* **2016**, *57*, 369−375.
(63) Barthel, J.; Hetzenauer, H.; Buchner, R. Dielectric Relaxation of Aqueous Electrolyte Solutions. II. Ion-pair Relaxation of 1:2, 2:1, and 2:2 Electrolytes. *Ber. Bunsen-Ges. Phys. Chem.* **1992**, *96*, 1424−1432.
(64) Dote, J. L.; Kivelson, D. Hydrodynamic Rotational Friction Coefficients for Nonspheroidal Particles. *J. Phys. Chem. A* **1983**, *87*, 3889−3893.
(65) Zemaitis, J. F.; Clark, D. M.; Rafal, M.; Scrivner, N. C. *Handbook of Aqueous Electrolyte Thermodynamics: Theory & Application*; Wiley-AIChE: Hoboken, NJ, 1986.
(66) Sillen, L. G.; Martell, A. E. *Stability Constants of Metal-Ion Complexes*, Spec. Publcn. No. 17; Chem. Soc.: London, UK, 1964.
(67) Sillen, L. G.; Martell, A. E. *Stability Constants of Metal-Ion Complexes*, Supplement No. 1, Spec. Publcn. No. 25; Chem. Soc.: London, UK, 1971.
(68) Högfeldt, E. *Stability Constants of Metal-Ion Complexes, Part A: Inorganic Ligands*; Pergamon: Oxford, UK, 1982.
(69) Akilan, C.; May, P. M.; Hefter, G. T. A Potentiometric Study of the Association of Copper(II) and Sulfate Ions in Aqueous Solution at 25°C. *J. Solution Chem.* **2014**, *43*, 885−892.
(70) Bond, A. M.; Hefter, G. T. Use of the Fluoride Ion Selective Electrode for the Detection of Weak Fluoride Complexes. *J. Inorg. Nucl. Chem.* **1971**, *33*, 429−434.
(71) Altounian, N.; Glatfelter, A.; Bai, S.; Dybowski, C. Thermodynamics of Ion Pairing in Lead Nitrate Solutions as Determined With ^{207}Pb NMR Spectroscopy. *J. Phys. Chem. B* **2000**, *104*, 4723−4725.
(72) Hefter, G. When Spectroscopy Fails: The Measurement of Ion Pairing. *Pure Appl. Chem.* **2006**, *78*, 1571−1586.
(73) Eberspächer, P.; Wismeth, E.; Buchner, R.; Barthel, J. Ion Association of Alkaline and Alkaline-earth Metal Perchlorates in Acetonitrile. *J. Mol. Liq.* **2006**, *129*, 3−12.
(74) Rohman, N.; Wahab, A.; Mahiuddin, S. Isentropic Compressibility, Shear Relaxation Time, and Raman Spectra of Aqueous Calcium Nitrate and Cadmium Nitrate Solutions. *J. Solution Chem.* **2005**, *34*, 77−94.

https://doi.org/10.1021/acs.jpcb.4c05441
J. Phys. Chem. B XXXX, XXX, XXX−XXX